Appl. Phys. A (2017) 123:562
DOI 10.1007/s00339-017-1174-0

Applied Physics A
Materials Science & Processing

Physical properties in polydomain *c/a/c/a* phase $PbTiO_3$ ferroelectric thick films: effect of thermal stresses

Gang Bai[1,2,3] · Xiaobing Yan[4] · Wei Li[1] · Cunfa Gao[2]

Received: 3 March 2017 / Accepted: 27 July 2017 / Published online: 1 August 2017
© Springer-Verlag GmbH Germany 2017

Abstract The thermal stress dependence of the physical properties of polydomain $PbTiO_3$ films on different substrates are investigated using a nonlinear Ginzburg–Landau–Devonshire thermodynamic model as a function of deposition temperature T_G and thermal expansion coefficients. It is found that the thermal strain has a large impact on the ferroelectric polarization states and other physical properties for the thicker ferroelectric thin films. Extrinsic contributions from 90° domain wall displacements are found to dramatically impact the dielectric, pyroelectric, and piezoelectric responses. Most importantly, the dielectric and piezoelectric constants in the polydomain *c/a/c/a* phase is much larger than that of the monodomain *c* phase, while the results are opposite for the ferroelectric polarization and pyroelectric coefficient. Careful choice of thermal stress and domain states allows one to harness the intrinsic and extrinsic contributions to obtain large physical responses. Our work is in good agreement with experimental results and phase–field simulation.

✉ Gang Bai
baigang@njupt.edu.cn

✉ Wei Li
liw@njupt.edu.cn

[1] College of Electronic Science and Engineering, Nanjing University of Posts and Telecommunications, Nanjing 210026, People's Republic of China

[2] State Key Laboratory of Mechanics and Control of Mechanical Structures, Nanjing University of Aeronautics and Astronautics, Nanjing 210016, People's Republic of China

[3] Laboratory of Solid State Microstructures, Nanjing University, Nanjing 210093, People's Republic of China

[4] College of Electronic and Information Engineering, Hebei University, Baoding 071002, People's Republic of China

1 Introduction

Thin film ferroelectrics are of great technological interest due to their potential applications in ferroelectric random access memories, dynamic random access memory, solid state cooling, etc. [1–5]. Prior studies are mostly focused on the misfit strain effect on the physical properties of monodomain ferroelectric thin films [6–9]. However, monodomain structures are stable only in ultrathin thin films, while thicker films possess the polydomain structures [10–12]. And for thick films, the misfit strain can be relaxed by the generation of misfit dislocations during film growth and annealing. So thermal stresses arising from different thermal expansion coefficients (TECs) between a film and substrate begins to dominate in absence of lattice-misfit strain in thicker films during cooling from growth temperature to ambient conditions. Thermal stresses have been minimally used to tune the physical properties of monodomain ferroelectric thin films. For example, thermal stresses result in *c*-axis-orientated $PbTiO_3$ (PTO) thin films grown on MgO (001) substrates despite the tensile nature of lattice-misfit strains [13]. In addition, thermal stresses can significantly impact the ferroelectric phase transition [14], and even tune dielectric, pyroelectric, piezoelectric and electrocaloric properties for epitaxial ferroelectric films [15–25]. However, a systematic theoretical study of thermal stress effects on the physical properties of polydomain ferroelectric thick films is still lacking. There is a real need for a mutual understanding of thermal stress dependence of the properties of polydomain ferroelectric thick films, which is necessary to satisfy their applications with improved design. In this paper, the Ginzburg–Landau–Devonshire thermodynamic theory is applied to investigate the effect of thermal strain on the dielectric, pyroelectric and piezoelectric properties in the polydomain

PTO thin films. Theoretical analysis shows that the dielectric, pyroelectric, and piezoelectric properties strongly depends on the substrates and deposition temperature T_G. The polydomain PTO thick films on MgO is expected to experience high thermal in-plane compressive strains due to the TECs mismatch, resulting in pyroelectric coefficients (absolute value), dielectric permittivity lower than the same thick films on Si, $SrTiO_3$, c-Al_2O_3 and $LaAlO_3$ for which there is a in-plane tensile thermal stress. Compared to the same monodomain films on the same substrate, the polydomain PTO films have the higher dielectric and piezoelectric properties, but a lower pyroelectric response.

2 Thermodynamic analysis

Considering the formation of thermal strains during cooling from the growth/processing temperature (T_G) to room temperature, the in-plane thermal strain u_T due to different TECs between films and substrates can be calculated by [20]:

$$u_T = \int_{RT}^{T_G} (\alpha_F - \alpha_S) dT, \quad (1)$$

where α_F, α_S are the in-plane TECs of films and substrates, respectively. The TECs of the film materials PTO and the substrates (001) MgO, Si, c-sapphire, $SrTiO_3$, and $LaAlO_3$ used in our calculations are given in Table 1 from Refs. [20, 22].

Here, we consider a polydomain single crystalline $PbTiO_3$ film grown on some thick (001)-oriented cubic substrates. During cooling from the growth/processing temperature (T_G) to room temperature the paraelectric-to-ferroelectric and ferroelectric-to-ferroelectric phase transitions will take place, ferroelectric films can form complex domain structures to minimize electrostatic and elastic energies at lower temperatures. To identify the equilibrium state of the polydomain films, Koukhar and coworkers developed a thermodynamic theory of dense domain ferroelectric thin films [26, 27]. They think that the polarization and strain fields inside the domain bulk are homogeneous and the domain wall energies are negligible when the film thickness is much more than the domain wall width [28, 29]. The results are solid for thick films where the theoretically predicted domain structures have been observed experimentally [30, 31].

We use the generalized Helmholtz free-energy density F for a ferroelectric thin film to obtain the equilibrium physical properties. F can be written as a function of the polarization P_i, stresses σ_i and electric field E_i [26, 27]

$$\begin{aligned} F = {} & a_1(P_1^2 + P_2^2 + P_3^2) + a_{11}(P_1^4 + P_2^4 + P_3^4) + a_{33}P_3^4 \\ & + a_{12}(P_1^2P_2^2 + P_1^2P_3^2 + P_2^2P_3^2) + a_{111}(P_1^6 + P_2^6 + P_3^6) \\ & + a_{112}[P_1^4(P_2^2 + P_3^2) + P_3^4(P_1^2 + P_2^2) + P_2^4(P_1^2 + P_3^2)] \\ & + a_{123}P_1^2P_2^2P_3^2 + \frac{1}{2}s_{11}(\sigma_1^2 + \sigma_2^2 + \sigma_3^2) \\ & + s_{12}(\sigma_1\sigma_2 + \sigma_2\sigma_3 + \sigma_3\sigma_1) + \frac{1}{2}s_{44}(\sigma_4^2 + \sigma_5^2 + \sigma_6^2) \\ & - \frac{1}{2}\varepsilon_0(E_1^2 + E_2^2 + E_3^2) - E_1P_1 - E_2P_2 - E_3P_3, \end{aligned} \quad (2)$$

where σ_i are the internal mechanical stresses in the film, a_1, a_{ij}, and a_{ijk} are the dielectric stiffness and higher-order stiffness coefficients at constant stress, s_{ij} are the elastic compliances at constant polarization, and Q_{ij} are the electrostrictive constants of the paraelectric phase. The phenomenological coefficients used in this calculations can be obtained in Table 2.

For the polydomain states, the mean free-energy density $\langle F \rangle$ can be written as $\langle F \rangle = \phi F' + (1-\phi)F''$, where ϕ is the domain fraction of the first domain type and F' and F'' are the energy densities within the domains of the first and second type, respectively. The free energy is supplemented by the mechanical boundary conditions for the polydomain phases [26, 27] and is minimized to obtain the equilibrium polarizations and domain populations.

For PTO thick films, the equilibrium domain structure can possess any of three different phases as a function of strain and temperature: one monodomain c, two polydomain ($c/a/c/a$ and $a_1/a_2/a_1/a_2$) phases [26, 27]. The monodomain c phase is stable at compressive strains as in monodomain films. The $c/a/c/a$ polydomain structure (a mixture of c and a_1 or a_2 domains), has been observed experimentally for thick films (>10 nm) [32] when the effective misfit strain is tensile [33, 34].

For the $c/a/c/a$ domain structure, the average out-of-plane polarization is $\langle P_3 \rangle = \phi_c P_3$, where ϕ_c is the fraction

Table 1 Thermal expansion coefficients of thin film and substrates ($\times 10^{-6}$/°C)

$PbTiO_3$	11.86
MgO	13.47
Si	$3.725 \times \{1 - \exp[-5.88 \times 10^3 (T + 149)]\} + 5.548 \times 10^{-4} (T + 273)$
c-Al_2O_3	$8.026 + 8.17 \times 10^{-4} T - 3.279 \exp(-2.91 \times 10^{-3} T)$
$SrTiO_3$	11
$LaAlO_3$	10

Table 2 Data for PTO

T_0	479 °C
a_1	$3.8\ (T - T_0) \times 10^5$ J m/C^2
a_{11}	-7.3×10^7 J m^5/C^4
a_{111}	2.6×10^8 J m^9/C^6
s_{11}	8.0×10^{-12} m^2/N
s_{12}	-2.5×10^{-12} m^2/N
Q_{11}	0.089 m^4/C^2
Q_{12}	-0.026 m^4/C^2

of c domains. P_3 is the spontaneous polarization in c domain which has the same magnitude in a domain. The equilibrium domain fraction of c domains upon application of an electric field and thermal strain field can be calculated as

$$\phi_c = 1 - \frac{(s_{11} - s_{12})(u_T - Q_{12}P_3^2)}{s_{11}(Q_{11} - Q_{12})P_3^2} + \frac{E_3(s_{11}^2 - s_{12}^2)}{2s_{11}(Q_{11} - Q_{12})^2 P_3^3}. \tag{3}$$

The mean pyroelectric coefficient can be calculated as

$$\langle p \rangle = \frac{\mathrm{d}\langle P_3 \rangle}{\mathrm{d}T} = \phi_c \frac{\mathrm{d}P_3}{\mathrm{d}T} + P_3 \frac{\mathrm{d}\phi_c}{\mathrm{d}T}, \tag{4}$$

where

$$\frac{\mathrm{d}P_3}{\mathrm{d}T} = \frac{-P_3\left[a_0 - \frac{Q_{12}}{s_{11}}(\alpha_S - \alpha_F)\right]}{\left[a_1 - \frac{Q_{12}}{s_{11}}u_T + 6\left(a_{11} + \frac{Q_{12}^2}{2s_{11}}\right)P_3^2 + 15a_{111}P_3^4\right]} \tag{5}$$

$$\frac{\mathrm{d}\phi_c}{\mathrm{d}T} = \frac{2(s_{11} - s_{12})u_T}{s_{11}(Q_{11} - Q_{12})P_3^3}\frac{\mathrm{d}P_3}{\mathrm{d}T} - \frac{(s_{11} - s_{12})(\alpha_S - \alpha_F)}{s_{11}(Q_{11} - Q_{12})P_3^2} - \frac{3E_3(s_{11}^2 - s_{12}^2)}{2s_{11}(Q_{11} - Q_{12})^2 P_3^4}\frac{\partial P_3}{\partial T}. \tag{6}$$

To evaluate the dielectric and piezoelectric response, the film average polarization $\langle P_3 \rangle$ and out-of-plane strain $\langle u_3 \rangle$ should be computed as a function of the external electric field ($E_0 \to 0$). The small-signal dielectric constants ε_{33} ($E_0 \to 0$) and piezoelectric constants $\langle d_{33} \rangle$ can be calculated as

$$\varepsilon_{33} = \frac{\langle P_3 \rangle(E_3 = E_0) - \langle P_3 \rangle(E_3 = 0)}{\varepsilon_0 E_0} \tag{7}$$

$$\langle d_{33} \rangle = \frac{\langle u_3 \rangle(E_3 = E_0) - \langle u_3 \rangle(E_3 = 0)}{E_0} \tag{8}$$

$$\langle u_3 \rangle = \frac{2s_{12}}{s_{11} + s_{12}}u_T + \left(Q_{11} - \frac{2Q_{12}s_{12}}{s_{11} + s_{12}}\right)\phi_c P_3'^2 + \frac{Q_{12}s_{11} - Q_{11}s_{12}}{s_{11} + s_{12}}(1 - \phi_c)P_1''^2, \tag{9}$$

where P_3' and P_1'' are the polarization within the domains of the c domain and a domain, respectively.

3 Results and discussion

As seen in Fig. 1, TECs of Si, c-sapphire, and $LaAlO_3$, $SrTiO_3$ are smaller than that of the PTO films in the temperature range of our analysis, so the in-plane thermal strains for PTO films on those substrates are tensile (see Fig. 2), and the tensile thermal strain is increased with increasing T_G. Because of α_S (MgO) > α_F ($PbTiO_3$), u_T at room temperature is compressive for PTO on MgO, and its magnitude also increases with increasing T_G.

In the thermal strain range of our analysis, PTO films form the *c/a/c/a* domain structure. Figure 3 plots the average out-of-plane polarization of PTO films on different substrates as functions of T_G in 25–800 °C range. With increasing T_G, the fraction of the c domain increases at compressive thermal strains for MgO substrate, but decreases at tensile thermal strains for Si, $SrTiO_3$, $LaAlO_3$, c-Al_2O_3 substrates. At compressive thermal strains, both P_3 and the fraction Φ_c increase, so the mean polarization $\langle P_3 \rangle$ is enhanced. At tensile strains, P_3 decreases and the fraction Φ_c also decreases, therefore the mean polarization $\langle P_3 \rangle$ also decreases. As expected, the mean polarization $\langle P_3 \rangle$ is greater for PT on MgO (compressive) compared to PT on other substrates (tensile). The TECs mismatch between the film and the substrate is more pronounced for PT films on Si. Accordingly, the mean polarization of PT films on Si is found to be even more sensitive to T_G due to a build-up of a larger amount of tensile strain.

In Fig. 4, we plot the deposition temperature dependence of the out-of-plane pyroelectric coefficient of polydomain (a) and monodomain (b) PTO films on five kinds of substrates at room temperature. The pyroelectric coefficient for polydomain structure is calculated via Eqs. (4)–(6), taking into account the (thermal) strain, electric field, and

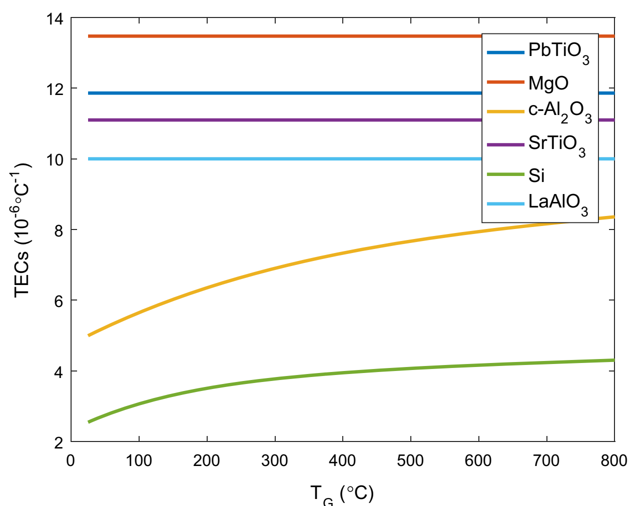

Fig. 1 Temperature dependence of the TECs of the substrates and ferroelectric material considered in this study

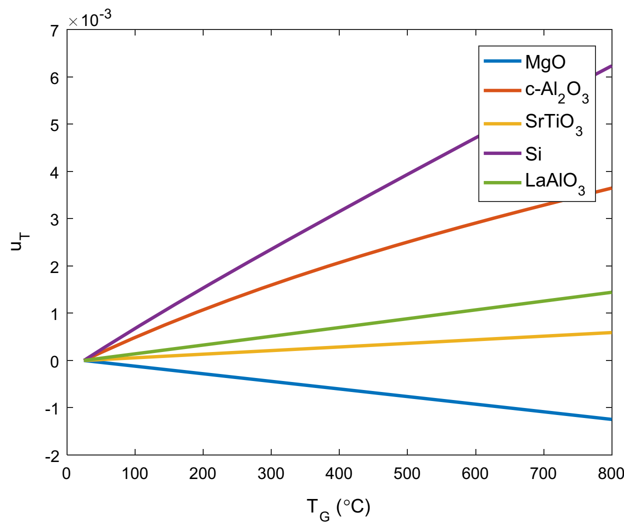

Fig. 2 Dependence of the thermal strains on the growth temperature for polydomain PTO on various substrates

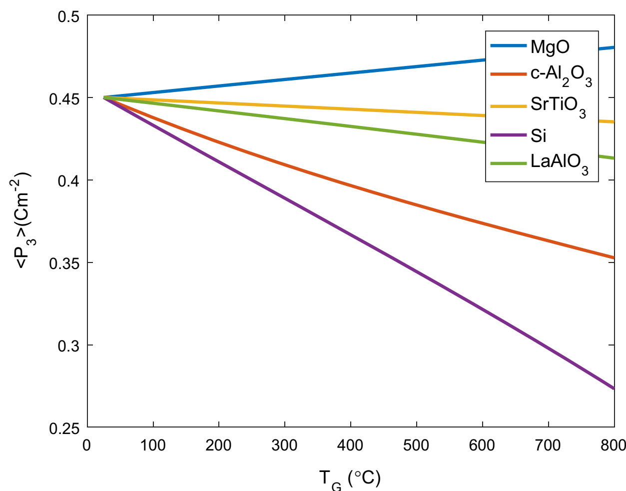

Fig. 3 Dependence of the mean polarization on T_G for PTO films on different substrates

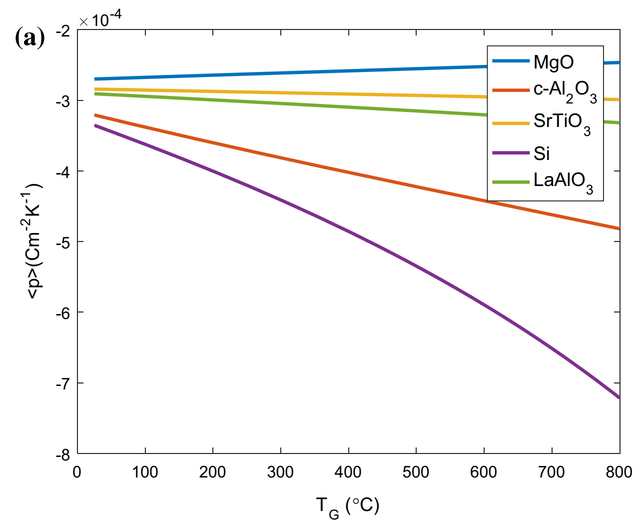

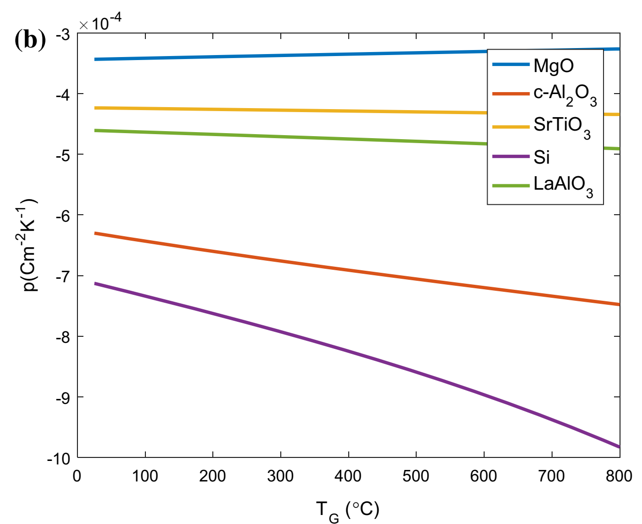

Fig. 4 The deposition temperature T_G dependence of pyroelectric response for polydomain (**a**) and monodomain (**b**) PTO films on Si, c-Al_2O_3, $LaAlO_3$, $SrTiO_3$ and MgO substrates

piezoelectric effect (the difference of TECs between substrates and films). In the previous works, we provided the analytical description of the out-of-plane pyroelectric coefficient for single-domain ferroelectric thin films, including the primary and secondary contributions [35, 36]. The primary contribution arises from a temperature-dependent change in the polarization of the bulk ferroelectrics. Since pyroelectric materials are also piezoelectrics, thermal expansion results in pyroelectricity which is referred to as a secondary contribution. In thin film ferroelectrics, this secondary contribution is related to the difference in TECs between the film and substrate. As a quantitative comparison with single-domain state, besides the above two effect, an extrinsic contribution to the primary pyroelectric coefficient is considered as shown in Eq. (6). The extrinsic contribution depends on domain wall motion driven by temperature, (thermal) strain and electric fields. However, in this work, we also analyze the contribution from piezoelectric effect to primary and extrinsic pyroelectric coefficient as shown in the second term of Eqs. (5) and (6), respectively. Since the fraction Φ_c is much lower than one, the magnitude of the mean out-of-plane pyroelectric coefficient of *c/a/c/a* structure is lower than that of monodomain *c* state. As the T_G increases, i.e., an increase in tensile thermal strain for Si, $SrTiO_3$, $LaAlO_3$, and c-Al_2O_3 substrates leads to the enhancement of the mean pyroelectric coefficients $\langle p \rangle$. For MgO substrate, the magnitude of the mean pyroelectric coefficients $\langle p \rangle$ is reduced since compressive thermal stain is enhance with increasing T_G.

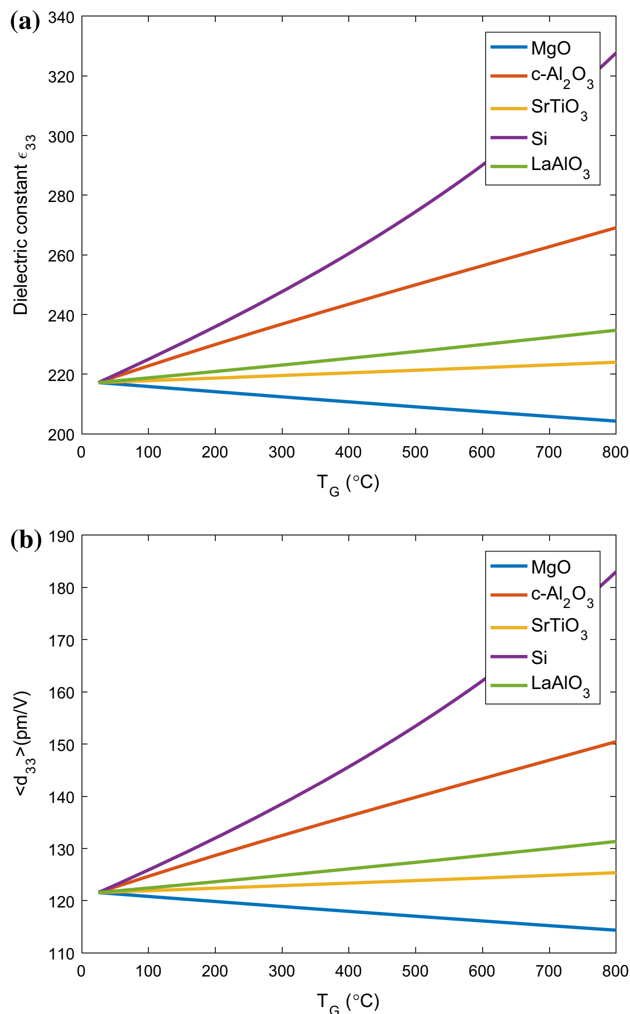

Fig. 5 Dependence of the mean dielectric (**a**) and piezoelectric (**b**) coefficients on T_G for polydomain PTO films on Si, *c*-Al_2O_3, $LaAlO_3$, $SrTiO_3$ and MgO substrates

Using Eqs. (7)–(9), we have performed numerical calculations of the out-of-plane permittivity ε_{33} and the out-of-plane piezoelectric constant $\langle d_{33} \rangle$, as shown in Fig. 5a, b. In the *c/a/c/a* structure the 90° domain wall contribution to the permittivity and piezoelectric responses are large. The out-of-plane polarization component P_3 differs in sign in the *c* (nonzero) and *a* domains (zero), so the electric field brings considerable driving force acting on the 90° domain walls. The electric field E_3 moves the 90° domain wall to *a* domain, which alters volumes and polarizations of *a* and *c* domains, so the extrinsic contribution from the 90° domain wall displacements also supports the mean polarization $\langle P_3 \rangle$ and strain $\langle u_3 \rangle$. Therefore, compared to the PTO monodomain films on the same substrate [20], the polydomain PTO films have the higher dielectric and piezoelectric properties due to the 90° domain wall displacements. For Si, $SrTiO_3$, *c*-Al_2O_3 and $LaAlO_3$ substrates inducing in-plane tensile thermal stresses, which suppress the polarization and the fraction of *c* domains, with the increase of T_G the dielectric and piezoelectric responses of PTO films are enhanced. Whereas for PTO films on MgO, compressive thermal stresses worsen the dielectric and piezoelectric responses with increasing T_G.

In the above calculations, we assume that the movement of the domain walls are free without any energy barriers. However, in reality the domain walls are pinned by the lattice imperfections or defects, which hinder their movement and reduce the extrinsic contribution [37, 38]. We also note that the polydomain microstructures can relax thermal stresses due to the TECs mismatch. So the extrinsic contribution to physical responses will be zero in the case of completely pinned domain walls, and in theory, our calculation places an upper bound on the extrinsic contribution to the physical properties. Beyond the motional extrinsic contribution from domain walls, various reports have highlighted the potential importance of a stationary or frozen contribution arising from the response of the volume of the ferroelectric material within the finite width of the domain walls to an applied stimulus irrespective of any lateral displacements or deformations of the wall [39–43]. The non-motional or stationary domain wall contribution to ferroelectric susceptibility has been proved to enhance the response [43]. Recent experimental results have demonstrated that the 90° domain walls displacements may extrinsically enhance the dielectric permittivity for low defect density ferroelectric films [44]. And phase–field simulations indicated that the dielectric constant ε_{33} has a larger value in tetragonal epitaxial ferroelectric films subjected to tensile biaxial strain with a large volume fraction of 90° domains [45]. These works are in good agreement with our model.

4 Conclusion

The dependence of the physical properties on thermally induced internal stress in polydomain PTO films on various substrates was analyzed via Landau–Devonshire thermodynamic model. Calculated results showed that the thermal stress can tune the mean polarization, dielectric and piezoelectric behaviors of polydomain PTO films remarkably. Compared to monodomain PTO films on the same substrate, the polydomain ferroelectric films have higher dielectric and piezoelectric properties due to the 90° domain wall displacements. This model shows the power of extrinsic contributions in enhancing dielectric and piezoelectric responses.

Acknowledgements This research was jointly supported by National Natural Science Foundation of China (Grant numbers of 51602159, 61674050 and 11472130), the China Postdoctoral Science Foundation (2016M590449), and the Jiangsu Province Postdoctoral Science Foundation (1601242C).

References

1. N. Setter, D. Damjanovic, L. Eng et al., J. Appl. Phys. **100**, 051606 (2006)
2. J.F. Scott, Science **315**, 954 (2007)
3. M. Dawber, K.M. Rabe, J.F. Scott, Rev. Mod. Phys. **77**, 1083 (2005)
4. J.F. Scott, Annu. Rev. Mater. Res. **41**, 1 (2011)
5. M. Valant, Prog. Mater. Sci. **57**, 980 (2012)
6. J.H. Haeni, P. Irvin, W. Chang, R. Uecker, P. Reiche, Y.L. Li, S. Choudhury, W. Tian, M.E. Hawley, B. Craigo, A.K. Tagantsev, X.Q. Pan, S.K. Streiffer, L.Q. Chen, S.W. Kirchoefer, J. Levy, D.G. Schlom, Nature **430**, 758 (2004)
7. K.J. Choi, M. Biegalski, Y.L. Li, A. Sharan, J. Schubert, R. Uecker, P. Reiche, Y.B. Chen, X.Q. Pan, V. Gopalan, L.-Q. Chen, D.G. Schlom, C.B. Eom, Science **306**, 1005 (2004)
8. N.A. Pertsev, A.G. Zembilgotov, A.K. Tagantsev, Phys. Rev. Lett. **80**, 1988 (1998)
9. D.G. Schlom et al., Annu. Rev. Mater. Res. **37**, 589 (2007)
10. G. Bai, W.H. Ma, Phys. B **405**, 1901 (2010)
11. Q.Y. Qiu, S.P. Alpay, V. Nagarajan, J. Appl. Phys. **107**, 114105 (2010)
12. A.R. Damodaran, J.C. Agar, S. Pandya, Z.H. Chen, L. Dedon, R. Xu, B. Apgar, S. Saremi, L.W. Martin, J. Phys. Condens. Matter **28**, 263001 (2016)
13. T. Ogawa, A. Senda, T. Kasanami, Jpn. J. Appl. Phys. **30**, 2145 (1991)
14. D. Tenne et al., Phys. Rev. B **69**, 2 (2004)
15. L.W. Martin, A.M. Rappe, Nat. Rev. Mater. **2**, 16087 (2016)
16. J. Karthik, L.W. Martin, Phys. Rev. B **84**, 024102 (2011)
17. J. Karthik, J.C. Agar, A.R. Damodaran, L.W. Martin, Phys. Rev. Lett. **109**, 257602 (2012)
18. D.M. Kim, C.B. Eom, V. Nagarajan, J. Ouyang, R. Ramesh, V. Vaithyanathan, D.G. Schlom, Appl. Phys. Lett. **88**, 142904 (2006)
19. Y.K. Kim, H. Morioka, R. Ueno, S. Yokoyama, H. Funakubo, K. Lee, S. Baik, Appl. Phys. Lett. **88**, 252904 (2006)
20. G. Bai, Z.G. Liu, X.B. Yan, C.C. Zhang, J. Appl. Phys. **116**, 054103 (2014)
21. M.T. Kesim, J. Zhang, S. Trolier-McKinstry, J.V. Mantese, R.W. Whatmore, S.P. Alpay, J. Appl. Phys. **114**, 204101 (2013)
22. Z.-G. Ban, S.P. Alpay, J. Appl. Phys. **91**, 9288 (2002)
23. G. Han, J. Ryu, W.H. Yoon, J.J. Choi, B.D. Hahn, J.W. Kim, D.S. Park, C.W. Ahn, S. Priya, D.Y. Jeong, J. Appl. Phys. **110**, 124101 (2011)
24. M.T. Kesim, J. Zhang, S.P. Alpay, L.W. Martin, Appl. Phys. Lett. **105**, 052901 (2014)
25. J. Karthik, A. Damodaran, L.W. Martin, Appl. Phys. Lett. **99**, 032904 (2011)
26. V.G. Koukhar, N.A. Pertsev, R. Waser, Phys. Rev. B **64**, 214103 (2001)
27. V.G. Kukhar, N.A. Pertsev, H. Kohlstedt, R. Waser, Phys. Rev. B **73**, 214103 (2006)
28. N.A. Pertsev, A.G. Zembilgotov, J. Appl. Phys. **78**, 6170 (1995)
29. N.A. Pertsev, A.G. Zembilgotov, J. Appl. Phys. **80**, 6401 (1996)
30. J.S. Speck, A. Seifert, W. Pompe, R. Ramesh, J. Appl. Phys. **76**, 477 (1994)
31. C.S. Ganpule, V. Nagarajan, B.K. Hill, A.L. Roytburd, E.D. Williams, R. Ramesh, S.P. Alpay, A. Roelofs, R. Waser, L.M. Eng, J. Appl. Phys. **91**, 1477 (2002)
32. S. Venkatesan, B.J. Kooi, J.T.M. De Hosson, A.H.G. Vlooswijk, B. Noheda, J. Appl. Phys. **102**, 104105 (2007)
33. B.S. Kwak, A. Erbil, J.D. Budai, M.F. Chisholm, L.A. Boatner, B.J. Wilkens, Phys. Rev. B **49**, 14865 (1994)
34. K. Lee, S. Baik, Annu. Rev. Mater. Res. **36**, 81 (2006)
35. G. Bai, D.M. Wu, Q.Y. Xie et al., J. Adv. Dielectr. **5**, 1550031 (2015)
36. G. Bai, Q.Y. Xie, Z.G. Liu, D.M. Wu, J. Appl. Phys. **118**, 074101 (2015)
37. F. Xu et al., J. Appl. Phys. **89**, 1336 (2001)
38. A.L. Kholkin et al., J. Appl. Phys. **89**, 8066 (2001)
39. W.N. Lawless, J.J. Fousek, Phys. Soc. Jpn. **28**, 419 (1970)
40. W.F. Rao, Y.U. Wang, Appl. Phys. Lett. **90**, 041915 (2007)
41. J. Hlinka, P. Ondrejkovic, P. Marton, Nanotechnology **20**, 105709 (2009)
42. A.N. Morozovska, E.A. Eliseev, O.V. Varenyk, S.V. Kalinin, J. Appl. Phys. **113**, 187222 (2013)
43. R.J. Xu, J. Karthik, A.R. Damodaran, L.W. Martin, Nat. Commun. **5**, 3120 (2014)
44. I. Vrejoiu et al., Adv. Mater. **18**, 1657 (2006)
45. Y.L. Li, S.Y. Hu, L.Q. Chen, J. Appl. Phys. **97**, 034112 (2005)